A Bayesian Model of Heart Rate to Reveal Real-time Physiological Information

Giorgio Quer and **Ramesh R. Rao**
Calit2 and Department of Electrical and Computer Engineering,
University of California, San Diego – La Jolla, CA 92093, USA

***Abstract*—The human heart rate is influenced by different internal systems of the body and can reveal valuable information about health and disease conditions. In this paper, we analyze the instantaneous heart rate signal using a Bayesian method, inferring in real time a probabilistic distribution that approximates the real distribution of this signal. The best model is chosen after an experimental analysis of real data collected within our framework. The parameters of this distribution can reveal interesting insights on the influences of the sympathetic and parasympathetic divisions of the autonomic nervous system (ANS) in real time.**

I. Introduction and Related Work

The frequency at which the human heart pulses (heart rate) is an important signal that can help in understanding not only the state of our heart, but the functioning of our internal systems [1], as well. It is possible to affect heart rate indirectly, through physical activity, emotions, and also through controlled breathing and other techniques. Heart rate is regulated by the interaction of the sympathetic and the parasympathetic nervous systems (SNS and PSNS, respectively), two branches of the autonomic nervous system (ANS). Parasympathetic innervation of the heart is controlled by the vagus nerve which acts to lower the heart rate by releasing a neurotransmitter called acetylcholine. On the other hand, the SNS increases heart rate, through the emission of two neurotransmitters: epinephrine (also known as adrenaline) and norepinephrine.

Motivated by this causal connection between the ANS and heart rate, a vast literature has focused on modeling heart rate variability (HRV), i.e., the cyclic and acyclic variations in the instantaneous heart rate (IHR), see e.g., [2]–[6]. The IHR is calculated each time a pulse is detected; it is inversely proportional to the time interval between two pulses. There is also a large body of literature on the clinical relevance of HRV, see e.g., the recent paper [7] and references therein. Regarding the connections between the HRV and the ANS, we refer the interested reader to [8] and references therein.

The mathematical methods adopted in the current literature can be divided into two typologies, the time-domain methods and the frequency-domain methods. The IHR is studied as a point process in [2], [3] and it is stochastically modeled as a history-dependent inverse Gaussian process, thus providing a new methodology for defining HRV in the time domain and analyzing it in both the time and frequency domains. Another interesting approach is presented in [4], where a phase-rectified signal averaging (PRSA) model is proposed. This method is suitable to study quasiperiodicity in nonstationary data; the paper highlights the advantages of this method over conventional spectral analysis. In [5] the PRSA is applied to a clinical trial where the method is shown to be effective as a predictor of mortality after myocardial infarction. This method is of particular interest since it discriminates between the acceleration and deceleration of the heart rate, thus distinguishing between the effects of the SNS and PSNS. From a medical point of view this is significant because it can reveal and specify important insights on the functioning of the ANS, which has an dramatic influence on both health and disease, see e.g., [9].

An overview of the literature reveals the importance of the heart rate signal as a key variable that is influenced by many internal processes and that can provide significant information about the health and/or disease status of a person. Many commercial sensors to detect the IHR are available to the public, therefore, we want to investigate if it is possible to analyze this signal with a simple device, e.g., a smartphone connected to the heart rate sensor, and what kind of information can be extracted from it. In addition, we want to investigate novel methods to extract information in real time from the heart rate signal, in order to give immediate feedback to the user regarding the effects of the activity that he/she is performing and the real-time reaction of his/her ANS.

In previous work [6], we have exploited the wavelet transformation to study the heart rate signal in the time-frequency domain. Using wavelet coherence [10], we were able to detect the presence of entrainment among people that are performing certain activities in unison.

In this paper, we propose a Bayesian analysis, with two levels of inference, to study the instantaneous variations in the heart rate. In particular, we propose a model that discriminates between the decrease and increase of the heart rate. We obtain a method that can be used to study in real time, with a simple nonobtrusive device, the individual effects of the two branches of the ANS (parasympathetic and sympathetic) on heart rate. The main contributions of this paper are:

- the study of the heart rate signal through a Bayesian method with two levels of inference;
- the use of this method for real-time updates of the signal distribution, each time a new heart pulse is recorded;
- the identification of a suitable model, based on real data analysis, to approximate such a signal;
- a preliminary real-time analysis of a heart-rate signal, with

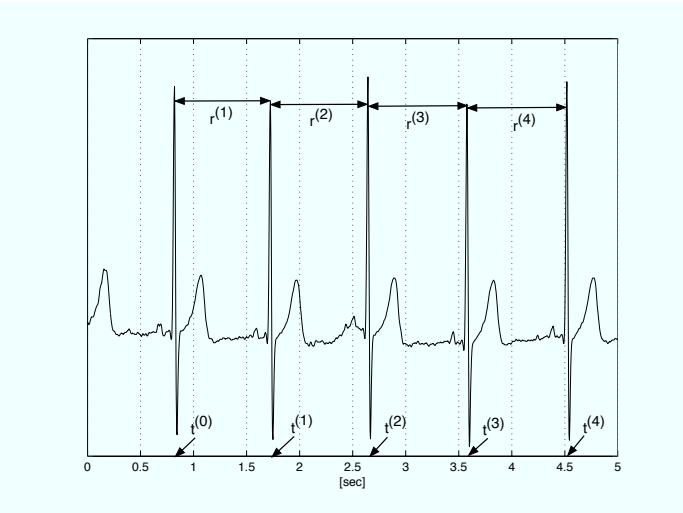

Figure 1. Electrocardiogram obtained from a BioHarness 3.0 device. In the figure we highlight the point process $\mathbf{t}$, the instants at which an R peak is detected, and $\mathbf{r}$, the intervals between peaks (RR intervals).

discrimination between heart rate increase and decrease, corresponding to the sympathetic and parasympathetic effects on the heart rate, respectively.

The rest of the paper is organized as follows. In Sec. II we briefly describe the data collection devices and the user interface developed for this project, then in Sec. III we detail the notation used to represent the heart rate signal. In Sec IV we present the Bayesian model adopted and optimized to infer a proper distribution for the heart rate signal, together with the techniques used to update such a distribution in real time. In Sec. V we select an appropriate model from real data analysis and we show preliminary results on the real-time analysis of the heart rate signal. Sec. VI provides a summary of the work.

II. Healthware platform

In this section we present the various tools for data collection and the user interface that we have developed at the University of California San Diego division of the California Institute for Telecommunications and Information Technology (Calit2): the Healthware platform [11]. The algorithms that will be described in detail in the following sections were developed using the data collected through this platform. The data analyzed in this paper were collected with two kinds of sensors.

- The Polar Team^2 Pro system: each device is composed of a chest strap, a sensor, and a transmitter. The devices are synchronized to a common internal clock and they are able to record information about the heart rate in the form of RR intervals, i.e., the time between two consecutive R peaks (pulses) of the heart signal. This signal is collected off-line via Bluetooth using the Polar Team^2 proprietary software on a central server that can be accessed from a personal computer via IEEE 802.11.
- The BioHarness 3.0: each device is composed of a chest strap, several sensors and a transmitter. It can sense the breathing rate (18 Hz), electrocardiography (ECG, up to 250 Hz), skin temperature, acceleration, and posture. It derives the RR intervals from the ECG. It can connect via Bluetooth to a personal computer, as well as a tablet or a smartphone, for real-time data visualization as well as off-line data collection.

The data collected can be visualized and analyzed on our Healthware website [11], where it is possible to analyze the available data with several time-domain [1] and frequency domain [6] data analysis tools optimized for the analysis of this kind of signal. The website is publicly available; users can upload their own data collected through a heart rate sensor, and analyze it with the available tools.

In addition, we are developing an Android application that can read the data from the BioHarness sensor via Bluetooth, visualize it in real time, pre-process the data, and send it to our website via IEEE 802.11. This application can run on a smartphone or tablet.

III. The continuos heart rate signal

In this section we detail the notation used to describe the heart rate signal sensed by the sensors, as well as the signals that are directly obtained from this data. The sensors are able to detect, with good accuracy, the time at which an R peak occurs, i.e., the peak in the electrocardiogram (ECG) shown in Fig. 1. The succession of the times at which an R peak is sensed can be represented as a point process, namely $\mathbf{t} = \mathbf{t}^{(0:N+1)}$, where $t^{(i)}$ is the time instant at which the i^{th} R peak is sensed, $i = 0, \ldots, N+1$. In order to analyze this random process we consider the process $\mathbf{r} = \mathbf{r}^{(1:N+1)}$ of the interarrival times between two consecutive pulses, namely:

$$r^{(i)} = t^{(i)} - t^{(i-1)} \,,$$

for all $i = 1, \ldots, N+1$. In the medical literature, $r^{(i)}$ is defined as an RR (or NN) time interval. From the process $\mathbf{r}$, it is possible to calculate the instantaneous heart rate (IHR) at time i (in pulses per minute), i.e.,

$$\mathrm{HR}^{(i)} = \frac{60}{r^{(i)}} \,.$$

In Fig. 2–(a) we represent each instance $r^{(i)}$ of the process as a function of the corresponding time $t^{(i)}$. Observing the figure, we can notice that the elements of $\mathbf{r}$ are not independent and identically distributed, instead, they strongly depend on the past history. An approach to analyze this kind of process that is often used by the medical community is to assume that each element of the process is independent, i.e., that $p\left[r^{(i)}|\mathbf{r}^{(1:(i-1))}\right] = p\left[r^{(i)}\right]$, where $\mathbf{r}^{(1:(i-1))}$ is the set of $r^{(j)}$, for $j = 1, \ldots, i-1$. Given this assumption, it is possible to estimate different statistics on $\mathbf{r}$, like the standard deviation [1], which can be calculated as:

$$\mathrm{SDNN} = \sqrt{\frac{\sum_{i=1}^{N}(r^{(i)})^2}{N} - \left(\frac{\sum_{i=1}^{N} r^{(i)}}{N}\right)^2} \,. \qquad (1)$$

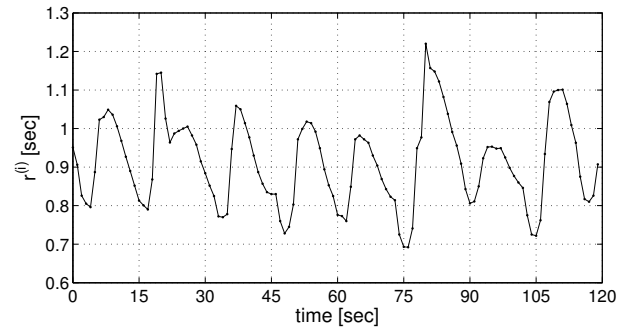

(a)

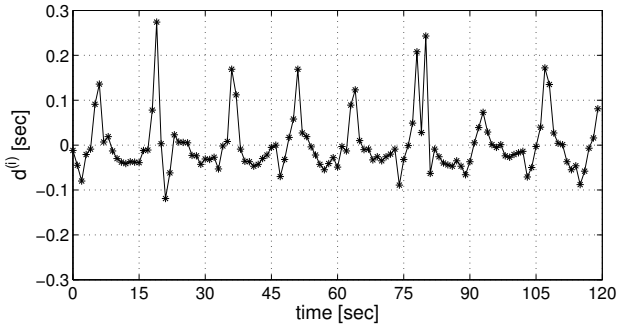

(b)

Figure 2. The RR interarrival times $\mathbf{r}$ (a), and the corresponding differences among the interarrival times $\mathbf{d}$ (b).

However, since each $r^{(i)}$ is strongly dependent on the recent history and the process $\mathbf{r}$ is not stationary, the measure of the SDNN can be very difficult to interpret from a statistical point of view. Another approach is based on the definition of another process, namely $\mathbf{d} = \mathbf{d}^{(1:N)}$, given by the differences between consecutive RR intervals, which is defined as:

$$d^{(i)} = r^{(i+1)} - r^{(i)} = t^{(i+1)} - 2t^{(i)} + t^{(i-1)} \ ,$$

for all $i = 1, \ldots, N$. An example of this process is shown in Fig. 2–(b).

In order to study the signal $\mathbf{d}$, it is common in the literature to implicitly assume that the interarrival times $\mathbf{r}$ are well approximated by a one step Markov process. In particular, we assume that each interarrival time $r^{(i)}$ is equal to the previous interarrival time $r^{(i-i)}$ plus an independent and identically distributed (i.i.d.) component, $d^{(i)}$. With this assumption, it is possible to study the distribution of such a process. Many interesting measures can be derived from this distribution, e.g., as presented in [12]:

$$\text{pNNx} = \frac{\sum_{i=1}^{N} \mathbb{1}\left(|d^{(i)}| \geq x\right)}{N} \simeq p\left(|d^{(i)}| \geq x\right) \ , \qquad (2)$$

where $\mathbb{1}(\cdot)$ is the indicator function. In the medical community the threshold is usually set to x = 50 ms, thus having only one measure for each process analyzed (the pNN50). This approach has some limitations, as detailed in [12], where the authors studied the pNNx measure for different values of x and suggested to use a value for the threshold as low as 20 ms, or less. This approach fails to discriminate between the increase ($d^{(i)} < 0$) and decrease ($d^{(i)} > 0$) of the instantaneous heart rate, because these two events are treated in the same way. Furthermore, the approach is limited to the choice of the threshold value x (a single determined value). In the next section, we propose a method to estimate the whole distribution of the differences between consecutive RR intervals, $\mathbf{d}$.

A. Removal of Artifacts

An important aspect to consider before proceeding with the analysis is the process of artifacts removal. The devices that are adopted in this study are equipped with proprietary software for artifacts removal. However, there are some artifacts that are not removed by the devices, but can be easily detected by observing $\mathbf{t}$ and $\mathbf{r}$. These can be fixed before proceeding with the analysis. Our artifact removal procedure is illustrated in pseudocode in Tab. I.

For every $i > P$

(1) Select the expected value based on the past P elements of $\mathbf{r}$

$$\hat{r}^{(i)} = \text{median}(\mathbf{r}^{(i-P:i-1)}) \ .$$

(2) If $r^{(i)} - \hat{r}^{(i)} > \alpha \hat{r}^{(i)}$ [Missing pulses detected]
add round$(r^{(i)}/\hat{r}^{(i)} - 1)$ equally spaced pulse arrivals between $t^{(i-1)}$ and $t^{(i)}$

(3) Else If $r^{(i)} - \hat{r}^{(i)} < -\alpha \hat{r}^{(i)}$ [Phantom pulse detected]
delete the pulse at $t^{(i)}$ if $t^{(i+1)} - t^{(i-1)} < t^{(i)} - t^{(i-2)}$, otherwise delete the pulse at $t^{(i-1)}$.

Table I
ALGORITHM TO REMOVE SOME OF THE ARTIFACTS FROM POINT PROCESS $\mathbf{t}$.

The effect of phase (2) is to lower bound the heart rate variability, since we substitute a long unrealistic interval with two or more equally sampled intervals. We stress that these artificial intervals are excluded from the Bayesian analysis of the heart rate variation in Sec. IV. The effect of phase (3) is to eliminate, where possible, a phantom pulse, thus restoring the real length of the interval at that point.

IV. A SIMPLE BAYESIAN MODEL FOR HEART RATE VARIATION

The heart rate signal is a nonstationary signal that can be represented by $\mathbf{t}$, $\mathbf{r}$, or $\mathbf{d}$, without loss of information. We can build a model that assumes that each instance of the interarrival time series is dependent only on the previous instance and on the state of the model, i.e.,

$$p\left[r^{(i)}|\mathbf{r}^{(1:(i-1))}, s^{(i)}\right] = p\left[r^{(i)}|r^{(i-1)}, s^{(i)}\right] \ , \qquad (3)$$

where $s^{(i)}$ is the state of the system at time i. Furthermore, we assume this process to be stationary in a short time interval, i.e.,

its state does not change in a short period of time, $s^{(i)} = s^\star$ for $i = 1, \ldots, N$. Under this assumptions we can write:

$$p\left[\mathbf{r}^{(1:N)}|s^\star\right] = \prod_{i=1}^{N} p\left[r^{(i)}|r^{(i-1)}, s^\star\right] \ . \tag{4}$$

We also assume that the differences between consecutive interarrival times are i.i.d., given that the state does not change, i.e.,

$$p\left[\mathbf{d}^{(1:N)}|s^\star\right] = \prod_{i=1}^{N} p\left[d^{(i)}|s^\star\right] \ . \tag{5}$$

Thus, it becomes possible to study the distribution of $d^{(i)}$, $p\left[d^{(i)}|s^\star\right]$, at least in the period in which the signal is stationary. To approximate this distribution, we adopt a standard Bayesian estimation method that relies on two levels of inference, similar to the approach detailed in [13] and applied in [14].

A. First Level of Bayesian Inference

We choose a set of M possible competitive models $\{\mathcal{M}_1, \ldots, \mathcal{M}_M\}$, and we rank them according to how well they approximate the distribution of $\mathbf{d}$. In particular, given the observed process $\mathbf{d}^{(1:N)}$, as a first step we maximize the posterior probability (Maximum A Posteriori, MAP) of the parameters $\boldsymbol{\theta}$ that describe each model, i.e., we find for each model $\mathcal{M}_j$:

$$\begin{aligned} \boldsymbol{\theta}_\star &= \arg\max_{\boldsymbol{\theta}} p\left(\boldsymbol{\theta}|\mathbf{d}^{(1:N)}, \mathcal{M}_j\right) \\ &= \arg\max_{\boldsymbol{\theta}} p\left(\mathbf{d}^{(1:N)}|\boldsymbol{\theta}, \mathcal{M}_j\right) \ , \end{aligned} \tag{6}$$

where the second equivalence holds because we do not have any prior information on the parameters distribution, i.e., $p(\boldsymbol{\theta}|\mathcal{M}_j)$ is constant for each value of $\boldsymbol{\theta}$ (non-informative prior). We obtain the best fitting parameter set for each model $\mathcal{M}_j$ considered.

B. Second Level of Bayesian Inference

In the second level of inference we select the model that best fits the data under consideration. Maximizing in an exhaustive way the probability of the model given the dataset is usually computationally very intensive, so we adopt a widely-used approximation to choose the best fitting model [15], i.e., the Bayesian Information Criterion (BIC), that in our case can be written as:

$$\mathrm{BIC}(\mathcal{M}_j) = \ln\left[p(\mathbf{d}^{(1:N)}|\boldsymbol{\theta}_\star, \mathcal{M}_j)p(\boldsymbol{\theta}_\star|\mathcal{M}_j)\right] - \frac{l_j}{2}\ln(N) \ , \tag{7}$$

where $\boldsymbol{\theta}_\star$ was defined in Eq. (6) and $l_j = \mathrm{size}(\boldsymbol{\theta}_\star)$ is the number of scalar parameters requested by the model $\mathcal{M}_j$. The BIC maximizes the likelihood of the data given the model and the best fitting parameters for such model, and at the same time it penalizes over the complexity of the model, expressed by the number of parameters l_j. In our case, under the stationary condition in Eq. (4), and given that the prior $p(\boldsymbol{\theta}_\star|\mathcal{M}_j)$ on the models' parameters is non-informative, we can simplify Eq. (7) and redefine the BIC as:

$$\mathrm{BIC}(\mathcal{M}_j) = \ln\left[\prod_{i=2}^{N} p(d^{(i)}|\boldsymbol{\theta}_\star, \mathcal{M}_j)\right] - \frac{l_j}{2}\ln(N) \ . \tag{8}$$

We will use such definition to rank the proposed models and choose the best fitting one.

C. Choice of the best fitting model

We propose eight different probabilistic models to fit the heart rate signal data that we collected in our experiments, each of which is completely described by one or two scalar parameters that can be calculated from the data using Eq. (6).

We have chosen the following four standard models to represent the data $\mathbf{d}^{(1:N)}$, where each of them has a different set of parameters $\boldsymbol{\theta}$:

- $\mathcal{M}_1 = \mathcal{L}_0$: a standard Laplacian model, with median $\mu = 0$ and $\theta = b$, the scale parameter,
- $\mathcal{M}_2 = \mathcal{G}_0$: a Gaussian model, with mean $m = 0$ and $\theta = \sigma$, the standard deviation,
- $\mathcal{M}_3 = \mathcal{L}$: a standard Laplacian model, with $\boldsymbol{\theta} = \{\mu, b\}$, the median and the scale parameter, respectively, and
- $\mathcal{M}_4 = \mathcal{G}$: a Gaussian model, with $\boldsymbol{\theta} = \{m, \sigma\}$, the mean and the standard deviation, respectively.

Since the observed distribution is significantly asymmetrical, we have also separated the dataset in two subsets:

$$\mathbf{d}_{<0} = \{d^{(i)} \text{ s.t. } d^{(i)} < 0\} \ , \tag{9}$$

and

$$\mathbf{d}_{\geq 0} = \{d^{(i)} \text{ s.t. } d^{(i)} \geq 0\} \ . \tag{10}$$

We propose the following models, that adopt a different distribution for the two subsets. We can fit the data with:

- $\mathcal{M}_5 = \mathcal{L}\mathcal{L}$: two Laplacian models,[1] with $\mu = 0$ and $\boldsymbol{\theta} = \{b_{<0}, b_{\geq 0}\}$, the two scale parameters,
- $\mathcal{M}_6 = \mathcal{G}\mathcal{G}$: two Gaussian models, with $m = 0$ and $\boldsymbol{\theta} = \{\sigma_{<0}, \sigma_{\geq 0}\}$, the two standard deviations,
- $\mathcal{M}_7 = \mathcal{L}\mathcal{G}$: one Laplacian model for $\mathbf{d}_{<0}$ and one Gaussian model for $\mathbf{d}_{\geq 0}$, with $\mu = m = 0$ and $\boldsymbol{\theta} = \{b_{<0}, \sigma_{\geq 0}\}$, and
- $\mathcal{M}_8 = \mathcal{G}\mathcal{L}$: one Gaussian model for $\mathbf{d}_{<0}$ and one Laplacian model for $\mathbf{d}_{\geq 0}$, with $\mu = m = 0$ and $\boldsymbol{\theta} = \{\sigma_{<0}, b_{\geq 0}\}$.

For each model, we estimate the parameters $\boldsymbol{\theta}$, according to Eq. (6), i.e., we find the MAP for each parameter, given that we have non-informative priors. In particular, the parameters that can be estimated from all the elements $d^{(i)}$ in the dataset $\mathbf{d}^{(1:N)}$, are, for the Laplacian distribution, the median μ of the points $d^{(i)}$, and the scalar parameter b that can be calculated as:

$$b = \frac{1}{N}\sum_{i=1}^{N} |d^{(i)} - \mu| \ ; \tag{11}$$

[1]The first model fits the data in $\mathbf{d}_{<0}$ with the parameter $b_{<0}$, the second model fits the data in $\mathbf{d}_{\geq 0}$ with the parameter $b_{\geq 0}$; in a similar way we can calculate the parameters for the models $\mathcal{M}_6$, $\mathcal{M}_7$, and $\mathcal{M}_8$.

and for the Gaussian distribution, $m = 1/N \sum d^{(i)}$, and σ, the standard distribution, calculated as:

$$\sigma = \sqrt{\frac{1}{N-1}\sum_{i=1}^{N}(d^{(i)} - m)^2} \ . \tag{12}$$

The calculation of the parameters in the case of a different distribution for the two datasets ($\mathbf{d}_{<0}$ and $\mathbf{d}_{\geq 0}$) is straightforward.

D. Real-time Model Update

An important feature common to all the models presented is that they are fully described by only one or two parameters, and it is possible to update such parameters in real time, every time a pulse is received. We do not consider in the following the models $\mathcal{M}_3$ and $\mathcal{M}_4$, that require also the update of the median and of the mean, respectively.[2] Specifically, we want to approximate the parameters of the distribution at the moment of the observation and we want to track how they evolve as a function of time. Thus, we consider only a limited amount, Q, of past elements, i.e., at time n we calculate the parameters of interest using only the elements $d^{(i)}$, with $i = n-Q+1, \ldots, n$. We refer to the scalar parameter of the Laplacian distribution calculated at time n as $b^{(n)}$ and to the standard deviation of the Gaussian distribution as $\sigma^{(n)}$, while for the models considered $m = \mu = 0$. At time $n+1$, we can update the parameter $b^{(n)}$ as:

$$b^{(n+1)} = b^{(n)} + \frac{|d^{(n+1)}| - |d^{(n-Q+1)}|}{Q} \ , \tag{13}$$

and the parameter $\sigma^{(n)}$ as:

$$\sigma^{(n+1)} = \sqrt{(\sigma^{(n)})^2 + \frac{(d^{(n+1)})^2 - (d^{(n-Q+1)})^2}{Q-1}} \ . \tag{14}$$

The generalization of the real-time update to the case of a different distribution for the two datasets ($\mathbf{d}_{<0}$ and $\mathbf{d}_{\geq 0}$) is straightforward.

We observe that after the initial calculations needed to estimate the parameters for the first time, their update requires only simple operations whose complexity does not depend on Q, the size of the considered dataset. This makes it possible to implement and run these techniques in real-time in devices with limited computation capabilities, or strong resource constraints, such as smartphones.

V. Results

In this section we exploit the mathematical framework detailed in Sec. IV to find a proper model for the heart rate data collected during our experiments. Then we will use this model to approximate in real time the distribution of the heart rate and to extract relevant information from this distribution. The data has been collected during different Kundalini yoga sessions and a Restorative yoga session, all performed at Calit2. Kundalini yoga [16] is a traditional meditation technique that involves controlled breathing and specific movements; it is performed in a group guided by a professional instructor. Restorative yoga is particularly indicated for relaxation and it is used to trigger the parasympathetic nervous system. As an example, we visualize the best fitting model for a single heart rate dataset from a Kundalini yoga session in Fig. 3. In this figure we have represented the distribution of the data collected with an histogram, and have calculated the best parameters for model $\mathcal{M}_1 = \mathcal{L}_0$ and $\mathcal{M}_2 = \mathcal{G}_0$. We can see from this example that the Laplacian model seems to fit the data significantly better than the Gaussian model, as will be confirmed by the following experimental analysis.

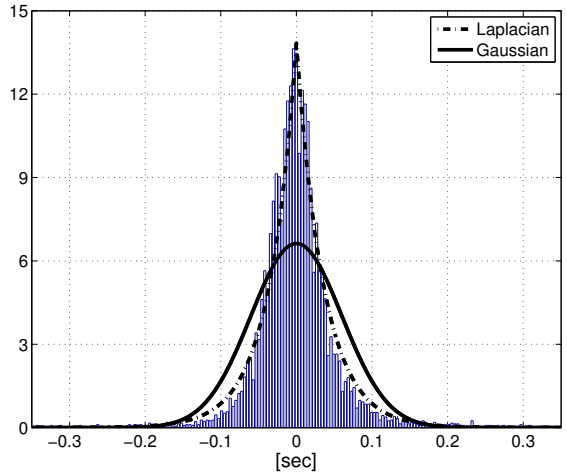

Figure 3. Empirical distribution and MAP best fitting for model $\mathcal{M}_1$ and for model $\mathcal{M}_2$, Laplacian and Gaussian distribution with zero mean, respectively.

A. Model Fitting

We have selected from our databases [11] a set of 34 heart rate time series, from six sessions of Kundalini yoga and one session of Restorative yoga. Each time series represents the heart rate signal of one person for the duration of the yoga session, approximately two hours. We have also analyzed two long heart rate signals (each longer than five hours), one during sleeping and one during an overnight flight, in order to have a richer set of signals to analyze.

We have applied the two-levels Bayesian inference to these time series and, for each signal analyzed, we have calculated the BIC according to Eq. (8). In Tab. II we show the BIC value for each dataset and for each model, averaged over all the subjects in the dataset. From the table, we can see that the best fitting model, for all heart rate signal sets, is the model $\mathcal{M}_5 = \mathcal{L}\mathcal{L}$, although the difference with $\mathcal{M}_1 = \mathcal{L}_0$ and $\mathcal{M}_3 = \mathcal{L}$ is minimal for some sets. We decided to adopt this model because it is the model that fits best with the available datasets, and because it gives us valuable information on the heart rate, discriminating between the increase and decrease of

[2]The median μ can not be updated with few simple operations. We do not deal with the real-time update of these two models, since they will not be adopted in Sec. V-B.

	$\mathcal{M}_1 = \mathcal{L}_0$	$\mathcal{M}_2 = \mathcal{G}_0$	$\mathcal{M}_3 = \mathcal{L}$	$\mathcal{M}_4 = \mathcal{G}$	$\mathcal{M}_5 = \mathcal{LL}$	$\mathcal{M}_6 = \mathcal{GG}$	$\mathcal{M}_7 = \mathcal{LG}$	$\mathcal{M}_8 = \mathcal{GL}$
Kundalini Yoga 1	2096	1835	2097	1834	**2098**	1840	1980	1958
Kundalini Yoga 2	1498	1383	1501	1382	**1502**	1404	1434	1472
Kundalini Yoga 3	1501	1390	**1502**	1390	**1502**	1395	1442	1454
Kundalini Yoga 4	1767	1681	**1768**	1680	**1768**	1690	1723	1736
Kundalini Yoga 5	1985	1771	1986	1771	**1988**	1783	1882	1888
Kundalini Yoga 6	1143	1006	1147	1006	**1148**	1027	1084	1091
Restorative Yoga	1301	1139	1301	1138	**1302**	1141	1223	1219
Long Recording	5644	5046	5645	5046	**5647**	5057	5319	5386

Table II
BAYESIAN INFORMATION CRITERION (BIC) AVERAGED OVER THE DIFFERENT HEART RATE SIGNALS THAT ARE COLLECTED IN EACH SESSION, AS A FUNCTION OF THE PROBABILISTIC MODEL ADOPTED. FOR EACH SET OF SIGNALS, THE BEST FITTING MODEL IS HIGHLIGHTED (BOLD).

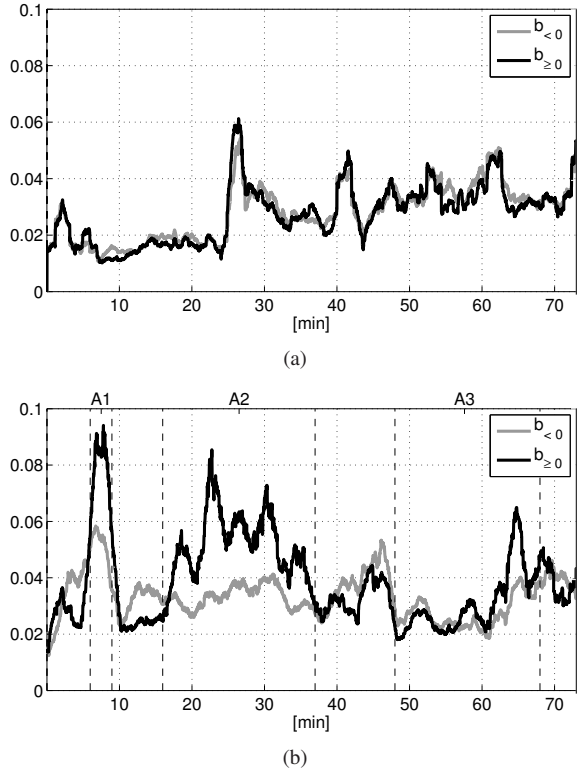

Figure 4. Scalar parameters of the Laplacian distribution, $\mathcal{M}_5 = \mathcal{LL}$: $b_{<0}$ (in light grey) and $b_{\geq 0}$ (in black) as a function of time during (a) rest, and (b) a Kundalini yoga meditation session.

the heart rate frequency. The increase in the heart rate frequency corresponds to a negative value for $d^{(i)}$, thus it is described by the parameter $b_{<0}$, while the decrease of the heart rate frequency corresponds to $d^{(i)} > 0$, and it is described by $b_{\geq 0}$. The former gives important information on the sympathetic response of the ANS, while the latter can help us understanding how the parasympathetic nervous system reacts. We stress the fact that this interpretation of the physiological meaning of these two parameters is based on the accepted hypothesis that the increase and decrease of the heart rate are directly caused by the sympathetic and parasympathetic branches of the ANS [1].

B. Real-time Parameters

In this section we apply the model identified in the previous section to track the time evolution of real instantaneous heart rate (IHR) data. Specifically, we calculate the two parameters of the chosen model, $b_{<0}$ and $b_{\geq 0}$, for a short period of time, $\Delta t = 120$ s, and we update the parameters each time a new pulse is recorded using Eq. (13). In Fig. 4 we show the evolution as a function of time for these two parameters, for the same subject while resting and during a Kundalini yoga session, in Fig. 4-(a) and Fig. 4-(b), respectively. During the Kundalini yoga session, the subject was involved in activities $A1$, $A2$, and $A3$, which are, in order, the Shoulder Shrug (an activity that involves a particular movement with the shoulders and hyperventilation), the Aad Sach Jugad Sach (an activity that involves the repetition of a Mantra, with the entire group in unison, coordinated by the instructor), and the Pratyhar Meditation (an activity that involves a particular movement of both arms). In Fig. 4–(b), we see the presence of a high peak for the parameter $b_{\geq 0}$ (the parameter related to the instantaneous decrease in the heart rate, thus related to the parasympathetic influence) during activity $A1$, then five peaks during the five phases of activity $A2$ and finally another peak at the end of activity $A3$. It is important to notice that, especially during activities $A1$ and $A2$, we are able to detect a strong asymmetry in the increase and decrease process. This effect is not seen when the subject is resting, in Fig. 4-(a).

This graphical representation can be seen as a tool to monitor the behavior of the parasympathetic ($b_{\geq 0}$) and the sympathetic ($b_{<0}$) influences of the ANS on the heart rate, with a nonobtrusive sensor device that can be used in everyday life and a simple visualization tool, like a smartphone, connected to the sensor.

VI. CONCLUSIONS AND FUTURE WORKS

In this paper we proposed a method to study the distribution of the differences among consecutive heart pulse interarrival times, fitting real data collected through our framework with the best fitting distribution model. We have shown how to update in real time the two parameters of the best fitting model, providing a real-time distribution for the signal. Furthermore, we have suggested a physiological interpretation of these two parameters, which correspond to the influences of the sympathetic and parasympathetic branches of the ANS.

Future works include the implementation of this model in a smartphone to give real-time feedback to the user on the state of his/her heart, as well as some insights on the behavior of the ANS. Furthermore, we plan to apply such technique in a more dynamic scenario, to study other physiological effects.

ACKNOWLEDGMENTS

The authors thank Maureen C. Curran for editorial assistance, the California Institute for Telecommunication and Technology (Calit2) for providing the environment for the experiments, and Qualcomm for the generous support.

REFERENCES

[1] Task Force of the European Society of Cardiology and the North American Society of Pacing Electrophysiology, "Heart Rate Variability: Standards of Measurement, Physiological Interpretation, and Clinical Use," *Circulation*, vol. 93, no. 5, pp. 1043–1065, 1996.

[2] G. Stanley, K. Poolla, and R. Siegel, "Threshold Modeling of Autonomic Control of Heart Rate Variability ," *Biomedical Engineering, IEEE Transactions on*, vol. 47, no. 9, pp. 1147–1153, Sept. 2000.

[3] R. Barbieri, E. C. Matten, A. A. Alabi, and E. N. Brown, "A point-process model of human heartbeat intervals: new definitions of heart rate and heart rate variability," *American Journal of Physiology: Heart and Circulatory Physiology*, vol. 288, no. 1, 2005.

[4] A. Bauer, J. W. Kantelhardt, A. Bunde, R. Schneider, M. Malik, and G. Schmidt, "Phase-rectified signal averaging detects quasi-periodicities in non-stationary data," *Physica A: Statistical Mechanics and its Applications*, vol. 364, pp. 423–434, 2006.

[5] A. Bauer, J. W. Kantelhardt, P. Barthel, R. Schneider, T. H. Mäkikallio, K. Ulm, K. Hnatkova, A. Schöning, H. V. Huikuri, A. Bunde, M. Malik, and G. Schmidt, "Deceleration capacity of heart rate as a predictor of mortality after myocardial infarction: cohort study," *American Journal of Physiology: Heart and Circulatory Physiology*, vol. 367, pp. 1674–1681, 2006.

[6] J. Daftari, G. Quer, and R. R. Rao, "Wavelet Coherence Reveals Entrainment of Heart Rate Variability Among People Involved in Group Activities," in *IEEE ICC*, Ottawa, Canada, June 2012.

[7] H. V. Huikuri and P. K. Stein, "Clinical Application of Heart Rate Variability after Acute Myocardial Infarction," *Frontiers in Physiology*, vol. 3, no. 41, 2012.

[8] L. D. DeBeck, S. R. Petersen, K. E. Jones, and M. K. Stickland, "Heart rate variability and muscle sympathetic nerve activity response to acute stress: the effect of breathing," *American Journal of Physiology: Regulatory, Integrative and Comparative Physiology*, vol. 299, no. 1, 2010.

[9] K. J. Tracey, "Physiology and immunology of the cholinergic antiinflammatory pathway," *The Journal of Clinical investigation*, vol. 117, no. 2, pp. 1043–1065, 2007.

[10] E. Cohen and A. Walden, "A statistical study of temporally smoothed wavelet coherence," *Signal Processing, IEEE Transactions on*, vol. 58, no. 6, pp. 2964 –2973, June 2010.

[11] A. Ganguly, R. Huang, G. Quer, and R. R. Rao, "HealthWare, Calit2, UCSD," Last accessed: August 2012. [Online]. Available: http://healthware.ucsd.edu/

[12] J. E. Mietus, C.-K. Peng, I. Henry, R. L. Goldsmith, and A. L. Goldberger, "The pNNx files: re-examining a widely used heart rate variability measure," *Heart*, vol. 88, no. 4, pp. 378–380, 2002.

[13] D. J. MacKay, "Bayesian Interpolation," *Neural Computation Journal*, vol. 4, no. 3, pp. 415–447, May 1992.

[14] G. Quer, R. Masiero, G. Pillonetto, M. Rossi, and M. Zorzi, "Sensing, Compression and Recovery for WSNs: Sparse Signal Modeling and Monitoring Framework," *to appear in Wireless Communications, IEEE Transactions on*.

[15] G. Schwarz, "Estimating the Dimension of a Model," *The Annals of Statistics*, vol. 6, no. 2, pp. 461–464, 1978.

[16] D. Shannahoff-Khalsa, *Kundalini Yoga Meditation: Techniques Specific for Psychiatric Disorders, Couples Therapy, and Personal Growth*. W. W. Norton and Co. Inc., 2006.